Draft version May 2, 2019
Typeset using LaTeX **twocolumn** style in AASTeX62

Entrainment of low Mach number thermals in stratified domains

Evan H. Anders,[1,2] Daniel Lecoanet,[3] and Benjamin P. Brown[1,2]

[1] *Dept. Astrophysical & Planetary Sciences, University of Colorado – Boulder, Boulder, CO 80309, USA*
[2] *Laboratory for Atmospheric and Space Physics, Boulder, CO 80303, USA*
[3] *Stuff*

(Received May 2, 2019; Revised May 2, 2019; Accepted ??)

Submitted to ApJ

ABSTRACT

Keywords: hydrodynamics — turbulence — entrainment

1. INTRODUCTION

Recent observations of solar convection have revealed a convective conundrum. Power spectra have revealed weaker flows than anticipated at large length scales, calling into question the existence of so-called "giant cells" driven by deep convection which would manifest as powerful, large-scale motions at the solar surface. This discrepancy between theory and observations has called into question our fundamental understanding of convection, sparking fruitful investigations into the nature of convection in the Sun.

Spruit (1997) hypothesized that convective motions may be driven entirely by cool downflows at the surface of the Sun, and Brandenburg (2016) expanded upon this "entropy rain" hypothesis. Brandenburg's work includes a careful expansion of mixing length theory to incorporate flux contributions from nonlocal convective motions, and handles this theory in a horizontally-averaged sense. He includes some discussion of possible flow morphologies which could be manifestations of this entropy rain, and even includes some brief simulations of propogating Hill vortices. However, these simulations and discussions did not include include a fundamental piece of entropy rain: it is buoyant, and has an entropy deviation from the background atmosphere.

If entropy rain does evolve into downward propagating buoyant vortex rings, it is important to understand how buoyancy effects the filling factor of these basic convective elements. In the context of Earth's atmosphere, so-called "thermals" are thought to be the nucleus of cloud formation. Thermals are buoyant areas of fluid which evolve into propagating buoyant vortex rings, and their evolution in the Boussinesq limit have been well studied in the laboratory for decades (see e.g., CITE), and more recently have been studied through Direct Numerical Simulation (DNS) in the laminar and turbulent regime (Lecoanet & Jeevanjee 2018). One fundamental result of these studies of thermals is that they experience a large degree of entrainment: their size expands with height and their propagation velocity slows despite their buoyant nature. However, we do not know of a study in which the propagation of these thermals, and thus the nature of their entrainment, is affected by a significant atmospheric stratification.

In the absence of buoyantly-induced entrainment, Brandenburg (2016) suggests that the filling factor, f, of vortex rings should decrease like $f \propto \rho^{\alpha}$ for horizontal compression and $f \propto \rho^{\alpha}$ for spherical compression. On the other hand, the filling factor of Boussinesq thermals *increases* like $f \propto d$, where d is the depth propagated. In this work, we extend the study of Lecoanet & Jeevanjee (2018) to study the propagation of low-Mach number, cold thermals in stratified domains, and how buoyant entrainment affects the scaling of their filling factor with depth. If buoyant entrainment is a dominant effect, it is possible that these buoyant vortex rings would simply grow too large and stall before reaching the bottom of the solar convection zone. On the other hand, if the compression effects suggested by Brandenburg (2016) are the dominant effect, then it is possible that these thermals could propagate to the bottom of the solar convection zone, or potentially shrink to a sufficiently small size where thermal dissipation is significant.

Corresponding author: Evan H. Anders
evan.anders@colorado.edu

We lay out our work as follows. In section 2, we develop a theoretical description of thermals in a stratified domain. In section 3, we describe and verify the experiments conducted in this work. In section 4, we compare the results of our experiments to the theory developed in section 2. Finally, in section 5, we discuss what our results imply for the entropy rain hypothesis.

2. THEORY

2.1. *Phenomenological description of thermal evolution*

We show pictorally the evolution of a cold thermal from rest in Fig. 1. In Fig. 1a, the evolution of a thermal in a weakly stratified domain with $n_\rho = 0.5$ density scale heights is shown. In Fig. 1b, the evolution of a thermal in an appreciably stratified domain with $n_\rho = 3$ density scale heights is shown. While the initial conditions are identical in both domains (spherical specific entropy perturbations of the same magnitude whose diameters are 5% of the domain depth), and while in both cases the thermal quickly evolves into a propagating buoyant vortex ring, we find that the $n_\rho = 0.5$ case entrains and grows with depth, similarly to the Boussinesq regime. On the other hand, the $n_\rho = 3$ case has a radius which remains approximately constant over time, and it reaches the bottom of the domain in many fewer nondimensional freefall time units.

2.2. *Theoretical description of thermal evolution*

The evolution of thermals as buoyant vortex rings has been well described in the unstratified, Boussinesq limit for decades (as early as e.g., CITE, and see Lecoanet & Jeevanjee (2018) for other sources). Buoyant motions in the atmospheres of stars and planets are generally large enough to feel the atmospheric stratification, and therefore a more thorough tratment of the evolution of thermals in stratified domains is required to understand the nature of thermal entrainment in nature.

In this work, we focus on the non-dissipative, low Mach number regime, in which the ideal anelastic equations are a decent approximation to the fully compressible equations. In this regime, the buoyancy is directly proportional to the specific entropy. In the absence of diffusion, or in the limit where diffusivities are sufficiently small, the volume-integrated total entropy is constant,

$$B \equiv \int_{\mathcal{V}} \rho\, s\, dV = \text{const}, \tag{1}$$

where $s = c_V \ln T - R \ln \rho$ is the specific entropy, with c_V the specific heat at constant volume and R the ideal gas constant.

In a stratified domain, the hydrodynamic impulse is defined Shivamoggi (2010),

$$\boldsymbol{I} = \frac{1}{2}\int_{\mathcal{V}} \boldsymbol{x} \times (\nabla \times (\rho \boldsymbol{u}))dV, \tag{2}$$

where $\boldsymbol{x}$ is the position vector, $\boldsymbol{u}$ is vector velocity, ρ is density, and $\mathcal{V}$ is the volume being integrated over. Furthermore, changes in the impulse can be expressed

$$\frac{\partial \boldsymbol{I}}{\partial t} = \int_{\mathcal{V}} \frac{\partial}{\partial t}(\rho \boldsymbol{u})dV = B\hat{z} + S, \tag{3}$$

where S is a combination of surface terms that disappears upon appropriate boundary conditions on $\mathcal{V}$ (Shivamoggi 2010). As we have assumed that the buoyancy, B, is constant, we can straightforwardly integrate

$$I_z = Bt + I_0, \tag{4}$$

for some constant I_0.

(need to work through this section carefully). Assuming an adiabatically stratified atmosphere in hydrostatic equilibrium, the vertical momentum equation is

$$= -\partial_z \varpi + g\frac{S_1}{c_P}, \tag{5}$$

where w is vertical velocity, S_1 is specific entropy, ϖ is the reduced pressure, $D/Dt = \partial_t + (\boldsymbol{u}\cdot\nabla)$ is the (eulerian? lagrangian?) derivative, g is gravity, and c_P is the specific heat at constant pressure. In the anelastic approximation, the density stratification is constant in time. OH GOD I DON'T KNOW THIS MATH WELL MAGIC MAGIC MAGIC. By doing magic, we arrive at

$$P_z = \beta B t + P_0. \tag{6}$$

Under the assumption that the thermal develops into a thin-core propagating vortex ring whose vortex core is radius r away from the axis of symmetry, the impulse can be approximated as $I_z \approx \pi\rho r^2 \Gamma$, where Γ is the circulation of the thermal vortex, which we assume to be constant. Rearranging, we find our first result,

$$r = \sqrt{\frac{Bt + I_0}{\pi\rho\Gamma}}. \tag{7}$$

In the limit where $\rho \to$ constant, as in the Boussinesq regime, we retrieve the $r \propto \sqrt{t}$ scaling found in the Boussinesq regime by Lecoanet & Jeevanjee (2018). We find that the inclusion of stratification adds the additional complexity of $r \propto \rho^{-1/2}$, such that downward-propogating vortex rings (as studied here) will not entrain to the same degree as boussinesq thermals, and upward-propogating rings will entrain more.

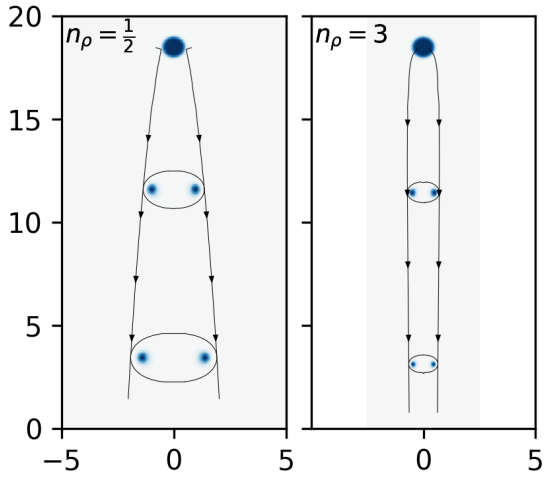

Figure 1.

We further assume that the volume-integrated momentum, $P_z \approx \rho V w_{th}$, where w_{th} is the vertical velocity of the thermal as a whole, and the volume of the fluid region propogating with the thermal is a spheroid, $V = V_0 r^3$, for some constant V_0. Plugging Eqn. 7 into this approximation, we find that

$$\rho^{-1/2} w = \left(\frac{(\pi\Gamma)^{3/2}}{V_0}\right) \frac{\beta B t + M_0}{(Bt + I_0)^{3/2}}. \tag{8}$$

Substituting $w = dz/dt$ and $\tau \equiv (Bt+I_0)/\Gamma$, We retrieve

$$\frac{dz}{\sqrt{\rho(z)}} = \left(\frac{\pi^{3/2}\Gamma}{V_0}\right)\left(\beta\Gamma\tau^{-1/2} + [M_0 - \beta I_0]\tau^{-3/2}\right) d\tau. \tag{9}$$

If the atmospheric stratification in which the thermal is falling is known, this result can be straightforwardly integrated with $\rho(z)$ plugged in in order to find the position of the thermal versus time. While we will leave this result general for now, we will plug in our polytropic stratification at the end of section 3, and show that the resulting expression does a good job of explaining the evolution of thermals in these atmospheres in section 4.

3. EXPERIMENT

3.1. *Anelastic Simulations*

In this work, we primarily study the evolution of 2D, azimuthally symmetric, anelastic thermals in cylindrical coordinates. We later verify that these simulations produce the same results a 3D fully compressible simulations in 3D cartesian domains (see sec. REF). The LBR anelastic equations are (Lecoanet et al. 2014),

$$\widetilde{\nabla}\cdot\widetilde{\boldsymbol{u}} = -\widetilde{w}\partial_{\tilde{z}}\ln\rho_0 \tag{10}$$

$$\frac{D\widetilde{\boldsymbol{u}}}{D\widetilde{t}} = -\widetilde{\nabla}\widetilde{\varpi} + g\frac{\widetilde{S_1}}{c_P}\hat{z} + \frac{1}{\rho_0}\widetilde{\nabla}\cdot\left(\mu\widetilde{\bar{\bar{\boldsymbol{\sigma}}}}\right) \tag{11}$$

$$\frac{D\widetilde{S_1}}{D\widetilde{t}} = \frac{1}{\rho c_P}\widetilde{\nabla}\cdot\left(\kappa T_0\widetilde{\nabla}\widetilde{S_1}\right) + \frac{\mu}{\rho_0 T_0}\widetilde{\sigma_{ij}}\partial_{\widetilde{x}_i}\widetilde{u}_j. \tag{12}$$

where terms with tildes are dimensional, and where $D/D\widetilde{t} = \partial/\partial\widetilde{t} + \widetilde{\boldsymbol{u}}\cdot\widetilde{\nabla}$. In our azimuthally symetric domain, we assume that $\partial_\phi = 0$; as the initial conditions of our simulations are at rest and have no azimuthal velocity, u_ϕ, we assume that $u_\phi = 0$; therefore $\boldsymbol{u} = u_r\hat{r} + w\hat{z}$. Under this approximation, the components of the stress tensor are

$$\begin{aligned}
&\widetilde{\sigma}_{rr} = 2\frac{\partial\widetilde{u_r}}{\partial\widetilde{r}} - \frac{2}{3}\widetilde{\nabla}\cdot\widetilde{\boldsymbol{u}}, \quad \widetilde{\sigma}_{rz} = \widetilde{\sigma}_{zr} = \frac{\partial\widetilde{w}}{\partial\widetilde{r}} + \frac{\partial\widetilde{u_r}}{\partial\widetilde{z}},\\
&\widetilde{\sigma}_{\phi\phi} = 2\frac{\widetilde{u_r}}{\widetilde{r}} - \frac{2}{3}\widetilde{\nabla}\cdot\widetilde{\boldsymbol{u}}, \quad \widetilde{\sigma}_{r\phi} = \widetilde{\sigma}_{\phi r} = 0,\\
&\widetilde{\sigma}_{zz} = 2\frac{\partial\widetilde{w}}{\partial\widetilde{z}} - \frac{2}{3}\widetilde{\nabla}\cdot\widetilde{\boldsymbol{u}}, \quad \widetilde{\sigma}_{\phi z} = \widetilde{\sigma}_{z\phi} = 0,
\end{aligned} \tag{13}$$

Furthermore, we assume that the dynamic viscosity, $\mu = \rho\nu$, and the thermal conductivity, $\kappa = \rho\chi$, are both uniform throughout the domain. The diffusivities ν and χ therefore scale inversely with the density.

We nondimensionalize these equations in the same manner as in Lecoanet & Jeevanjee (2018) such that the length scale is the diameter of the initial thermal perturbation and the velocity scale is the freefall velocity. The timescale is thus the freefall crossing time of

this unit length. Mathematically,

$$\begin{aligned} \widetilde{\nabla} \rightarrow (\widetilde{L}_{th}^{-1})\nabla, \qquad & \widetilde{S}_1 \rightarrow (\Delta\widetilde{S})S_1, \\ \widetilde{\boldsymbol{u}} \rightarrow (\widetilde{u}_{th})\boldsymbol{u}, \qquad & \widetilde{\varpi} \rightarrow (\widetilde{u}_{th}^2)\varpi, \\ \partial_{\tilde{t}} \rightarrow (\widetilde{u}_{th}/\widetilde{L}_{th})\partial_t, & \end{aligned} \tag{14}$$

with

$$\tilde{u}_{th}^2 = \frac{g\tilde{L}_{th}\Delta\tilde{s}}{c_P}, \qquad \mathrm{Re}_{\mathrm{ff}} = \frac{\tilde{u}_{th}\tilde{L}_{th}}{\nu}, \qquad \mathrm{Pr}_{\mathrm{ff}} = \frac{\tilde{u}_{th}\tilde{L}_{th}}{\chi}. \tag{15}$$

As the diffusivities scale with depth, $\mathrm{Re}_{\mathrm{ff}}$ is specified at the thermal's initial depth. The resulting equations are,

$$\nabla \cdot \boldsymbol{u} = -w\partial_z \ln\rho_0, \tag{16}$$

$$\partial_t \boldsymbol{u} + \boldsymbol{u}\cdot\nabla\boldsymbol{u} = -\nabla\varpi + S_1\hat{z} + \frac{1}{\mathrm{Re}_{\mathrm{ff}}}\left[\nabla^2\boldsymbol{u} + \frac{1}{3}\nabla(\nabla\cdot\boldsymbol{u})\right] \tag{17}$$

$$\partial_t S_1 + \boldsymbol{u}\cdot\nabla S_1 = \frac{1}{\mathrm{Re}_{\mathrm{ff}}}\left(\frac{1}{\mathrm{Pr}_{\mathrm{ff}}\rho_0 c_P}\left[\nabla^2 S_1 + \partial_z \ln T_0 \cdot \partial_z S_1\right] + \frac{-(\nabla_{ad})}{\rho_0 T_0}\sigma_{ij}\partial_{x_i}u_j\right) \tag{18}$$

where in this nondimensionalization, the adiabatic temperature gradient is defined in the next subsection.

3.2. *Atmosphere & Initial conditions*

We study an ideal gas whose equation of state is $P = \rho T$ and whose stratification is a perfectly adiabatic polytrope,

$$T_0 = 1 + (\nabla_{\mathrm{ad}})(z - L_z) \tag{19}$$

$$\rho_0 = T_0^{m_{\mathrm{ad}}}, \tag{20}$$

where $m_{\mathrm{ad}} = (\gamma-1)^{-1}$, and the adiabatic temperature gradient in these nondimensional atmospheres is

$$\nabla_{\mathrm{ad}} = -\frac{(e^{n_\rho/m_{ad}} - 1)}{L_z}\frac{m_{ad}+1}{c_P},$$

where L_z is the atmospheric depth in units of thermal diameters.

To initialize the simulation, we specify a spherical initial specific entropy perturbation,

$$S_1 = -A(1 - \mathrm{erf}\left(\frac{r' - r_{th}}{\delta}\right))/2, \tag{21}$$

where $A = 1$ for our scaled equations. Here, $r' = \sqrt{r^2 + (z-z_0)^2}$, where $z_0 = L_z - 3 * r_{th}$, with the thermal radius set as $r_{th} = 0.5$, and a smoothing width, $\delta = 0.1$.

3.3. *Fully Compressible Simulations*

In order to verify the validity of our 2D Anelastic simulations, we evolve select thermals according to the 3D Navier Stokes equations in a cartesian domain. We use the $(T, \ln\rho)$ formulation of the equations in which we have previously studied fully compressible convection at low and high Mach number (Anders & Brown 2017; Lecoanet et al. 2014),

$$\frac{D\ln\rho}{Dt} + \nabla\cdot\boldsymbol{u} = 0 \tag{22}$$

$$\frac{D\boldsymbol{u}}{Dt} = -\nabla T - T\nabla\ln\rho - g\hat{z} + \frac{1}{\rho}\nabla\cdot(\mu\bar{\bar{\boldsymbol{\sigma}}}) \tag{23}$$

$$\frac{DT}{Dt} + (\gamma-1)T\nabla\cdot\boldsymbol{u} = \frac{1}{\rho c_V}\nabla\cdot(\kappa\nabla T) + \frac{\mu}{\rho c_V}\sigma_{ij}\partial_{x_i}u_j. \tag{24}$$

where the viscous stress tensor is defined as

$$\sigma_{ij} = \left(\partial_{x_i}u_j + \partial_{x_j}u_i - \frac{2}{3}\delta_{ij}\nabla\cdot\boldsymbol{u}\right). \tag{25}$$

These equations are nondimensionalized on the temperature gradient length scale such that $\nabla_{\mathrm{ad}} = -1$ and the nondimensional timescale is the sound crossing time of that unit length.

In setting the specific entropy, $S = c_V\ln T - R^{-1}\ln\rho$, to an equivalent condition to that specified in Eqn. 21, we note that it is essential that the initial perturbation be in pressure equilibrium. The set of initial conditions that achieves this is

$$\ln\rho_1 = S_1/c_P, \qquad T_1 = T_0(e^{-\ln\rho_1} - 1). \tag{26}$$

We specify the magnitude of the initial entropy perturbations as $A = \epsilon = 10^{-4}$, such that the mach number of the resultant thermal is $\mathrm{O}(10^{-2})$ or less.

The depth of the atmosphere in these fully compressible domains is set by the number of density scale heights as $L_z = e^{n_\rho/m_{ad}} - 1$, and in order to compare results from these simulations to our nondimensionalized thermal simulations, we rescale all length scales in post-processing by $\ell = 20/L_z$, all timescales by $\tau = \sqrt{\ell\epsilon}$, and the entropy by $s = \epsilon^{-1}$.

3.4. *Solution for thermal evolution in a Polytrope*

Here we take the general theory described in Eqn. 27 and apply it to the specific case of the polytropes we study here. We note that, $\rho_0 = T_0^{m_{ad}}$ and $dT_0 = (\nabla_{\mathrm{ad}})dz$, such that we must solve

$$T_0^{-m_{ad}/2}dT_0 = \left(\frac{\pi^{3/2}\Gamma\nabla_{\mathrm{ad}}}{V_0}\right)\left(\beta\Gamma\tau^{-1/2} + [M_0 - \beta I_0]\tau^{-3/2}\right)d\tau. \tag{27}$$

Assuming that $m_{ad} < 2$ and through the use of simple power law integrals, we find that

$$T_0(t) = \left(C[\xi(\tau) - \xi(\tau_0)] + T_0(t_0)^{1/\alpha}\right)^{\alpha}, \tag{28}$$

with

$$\xi(\tau) = \beta\Gamma\tau^{1/2} - (M_0 - \beta I_0)\tau^{-1/2}, \tag{29}$$

$C \equiv (2\pi^{3/2}\Gamma(\nabla_{\rm ad}))/(\alpha V_0 B)$

3.5. *Verification of 2D Anelastic approximation*

blah blah blah comparison of 2D and 3D blah blah blah. z v t, r v z, w v z. Also side-by-side pictoral comparison with diff.

4. RESULTS

Picture of a big old grid of z v t, r v z, w v z.

Pretty picture showing thermal evolution (comparing low and high stratification).

Verification of theory by simulations

Table of found parameters for the fits

Two regimes: stalling and falling.

5. DISCUSSION

Wild speculation about extensions to the solar regime. Do things on the sun shrink to the point where they viscously dissipate?

Talk about what would happen if we were to study up-thermals.

Extensions, and the fact that we trust these results will likely hold in the solar regime.

This work was supported by NASA Headquarters under the NASA Earth and Space Science Fellowship Program – Grant 80NSSC18K1199. This work was additionally supported by NASA LWS grant number NNX16AC92G. Computations were conducted with support by the NASA High End Computing (HEC) Program through the NASA Advanced Supercomputing (NAS) Division at Ames Research Center on Pleiades with allocation GID s1647.

APPENDIX

A. THERMAL TRACKING

We use a thermal tracking algorithm very similar to the one used in Lecoanet & Jeevanjee (2018) and inspired by the work of **?**.

We begin by measuring the thermal's height versus time. To do so, we average the domain's entropy profile in radius and azimuth to create an average profile of entropy with height, and then we use scipy's brentq function on the derivative of that profile to find its maximum.

Next, we find the best fit of the thermal's height vs. time according to our theory and derive that fit according to Eqn. **??** to find the bulk vertical velocity of the thermal, w_b. We then calculate the streamfunction of the velocity field as in **?**,

$$\frac{\partial\psi}{\partial r} = 2\pi\rho r(w - w_b), \tag{A1}$$

with the boundary condition that $\psi = 0$ at $r = 0$. The contour defined by $\psi = 0$ from this solution is taken to be the outline of the thermal, and the volume of the thermal is taken to be the volume radially inward from that contour.

B. TABLE OF SIMULATIONS

REFERENCES

Anders, E. H., & Brown, B. P. 2017, Physical Review Fluids, 2, 083501

Brandenburg, A. 2016, ApJ, 832, 6

Lecoanet, D., Brown, B. P., Zweibel, E. G., et al. 2014, ApJ, 797, 94

Lecoanet, D., & Jeevanjee, N. 2018, arXiv e-prints, arXiv:1804.09326

Shivamoggi, B. K. 2010, Physics Letters A, 374, 4736

Spruit, H. C. 1997, Mem. Soc. Astron. Italiana, 68, 397

Table 1. Table of simulation information

n_ρ	$L_{thermal}/H_\rho$	nr or nx = ny	nz	$t_{evolution}$	safety
2D Anelastic Simulations					
0.1		128	512	45	100
0.5		128	512	45	100
1		128	512	45	100
2		256	512	30	100
3		512	1024	30	100
4		1024	1024	30	100
5					
6					
7					
3D Fully Compressible Simulations					
0.5		256	512	45	0.6
1		256	512	45	0.6
2		256	1024	45	0.6
3		256	2048	45	0.6

NOTE—